REAL-TIME FUSED COLOR IMAGERY FROM TWO-COLOR MIDWAVE HgCdTd IRFPAS

August 1998

James R. Waterman and Dean Scribner
Naval Research Laboratory
Washington, DC 20375

ABSTRACT

Real time display of color imagery has been demonstrated using a two-color midwave HgCdTe IRFPA built by Raytheon SBRC. A variety of algorithms were implemented using a real time image processor (TI C80) on a PC based frame grabber board. Statistically based scaling, de-correlation, spectral band differencing, and histogram equalization have been applied using the red-cyan color space representation of the imagery.

1.0 INTRODUCTION

Two-color midwave IRFPAs are being developed for missile approach warning sensors[1], which perform target identification using an autonomous processor. The high degree of correlation between 300 K thermal signatures for the two closely spaced bands, makes the spectral discrimination of spectrally sharp non-thermal, (e.g. CO2 emission) or high temperature, (e.g. solar reflection) sources possible using a simple weighted difference of the two bands. In spite of the closeness of the bands however, there are still emissivity and reflectivity related color differences for nominally graybody objects, which can form the basis for color display of the information. This work investigates the performance of two color midwave focal planes as imaging sensors with real time color display to aid in visual feature identification. Real time display of color imagery formed by fusing information from a two-color midwave HgCdTe IRFPA built by Raytheon SBRC, using a variety of algorithms implemented in a real time processor (TI C80) on a PC based frame grabber has been demonstrated for the first time. Statistically based scaling, spectral band differencing, and histogram equalization have been applied using the red-cyan color space representation of the imagery.

2.0 IRFPA PERFORMANCE CHARACTERIZATION

The two color midwave focal planes[2] have been characterized while operating at a 60Hz frame rate in a 50 mm focal length f/2.3 camera (SEIR Inc) at 80K. The focal planes have approximate cutoff wavelengths of 4.0 and 4.5 microns, and exhibit spectral cross talk of less than 5% away from the crossover region (**Figure 1**). The cut-on wavelength for the shorter band was defined by a warm dewar window and was 3.3 microns. The mean FPA digital outputs for integration times of 2.0 and 3.0 msec for the short and long band respectively, are shown as a function of blackbody temperature in **Figure 2.** Responsivities of 51 and 76 counts/K were

REPORT DOCUMENTATION PAGE

Form Approved OMB No. 0704-0188

1. REPORT DATE (DD-MM-YYYY)
01-08-1998

2. REPORT TYPE
Conference Proceedings

3. DATES COVERED (FROM - TO)
xx-xx-1998 to xx-xx-1998

4. TITLE AND SUBTITLE
Real-Time Fused Color Imagery From Two-Color Midwave HgCdTd IRFPAS
Unclassified

5a. CONTRACT NUMBER

5b. GRANT NUMBER

5c. PROGRAM ELEMENT NUMBER

6. AUTHOR(S)
Waterman, James R. ;
Scribner, Dean ;

5d. PROJECT NUMBER

5e. TASK NUMBER

5f. WORK UNIT NUMBER

7. PERFORMING ORGANIZATION NAME AND ADDRESS
Naval Research Laboratory
Washington, DC20375

8. PERFORMING ORGANIZATION REPORT NUMBER

9. SPONSORING/MONITORING AGENCY NAME AND ADDRESS
Director, CECOM RDEC
Night vision and Electronic Sensors Directorate, Security Team
10221 Burbeck Rd.
Ft. Belvoir, VA22060-5806

10. SPONSOR/MONITOR'S ACRONYM(S)

11. SPONSOR/MONITOR'S REPORT NUMBER(S)

12. DISTRIBUTION/AVAILABILITY STATEMENT
APUBLIC RELEASE
,

13. SUPPLEMENTARY NOTES
See Also ADM201041, 1998 IRIS Proceedings on CD-ROM.

14. ABSTRACT
Real time display of color imagery has been demonstrated using a twocolor midwave HgCdTe IRFPA built by Raytheon SBRC. A variety of algorithms were implemented using a real time image processor (TI C80) on a PC based frame grabber board. Statistically based scaling, de-correlation, spectral band differencing, and histogram equalization have been applied using the red-cyan color space representation of the imagery.

15. SUBJECT TERMS

16. SECURITY CLASSIFICATION OF:

a. REPORT	b. ABSTRACT	c. THIS PAGE
Unclassified	Unclassified	Unclassified

17. LIMITATION OF ABSTRACT
Public Release

18. NUMBER OF PAGES
10

19. NAME OF RESPONSIBLE PERSON
Fenster, Lynn
lfenster@dtic.mil

19b. TELEPHONE NUMBER
International Area Code
Area Code Telephone Number
703767-9007
DSN
427-9007

Standard Form 298 (Rev. 8-98)
Prescribed by ANSI Std Z39.18

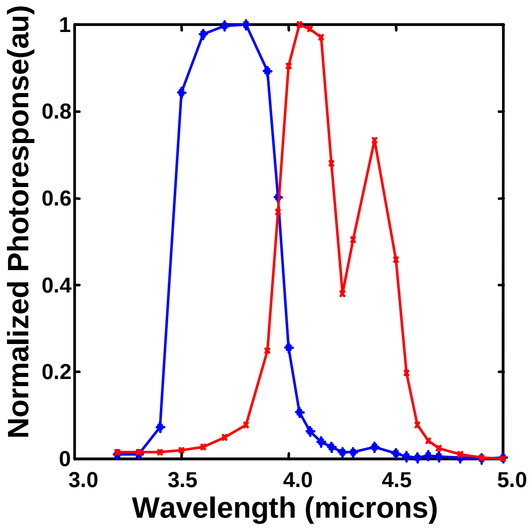

Figure 1 FPA spectral response

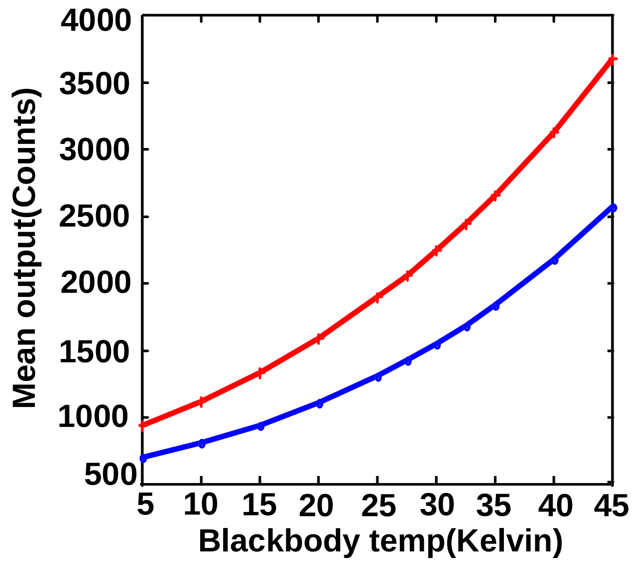

Figure 2 FPA blackbody responsivity for longer (red) and shorter (blue) bands.

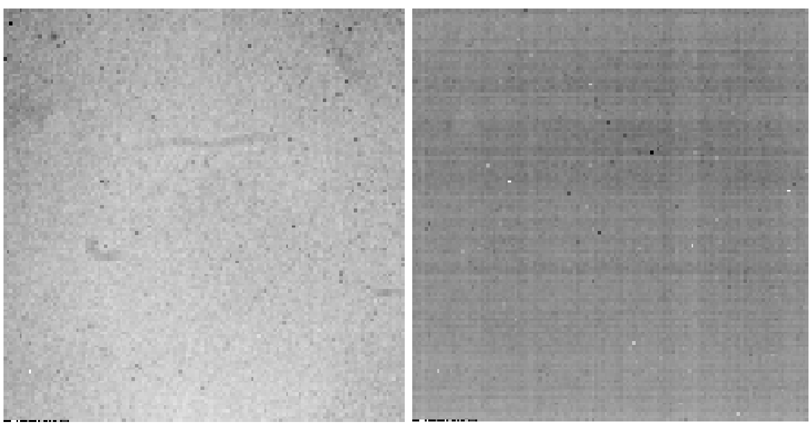

Figure 3 Responsivity (left) and offset (right) maps for MW1 (shorter) band

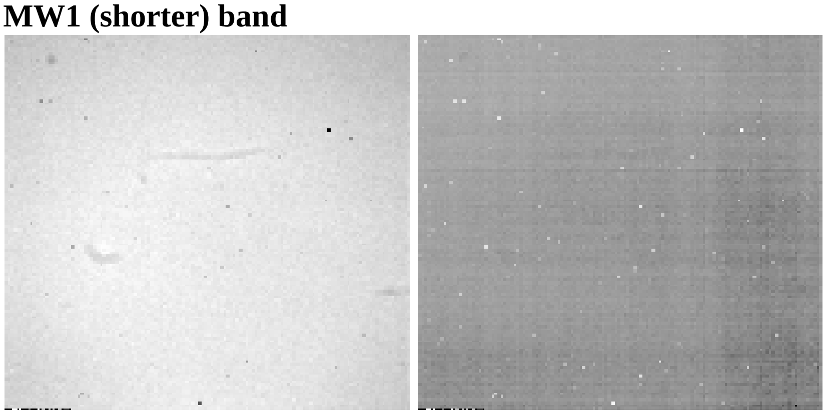

Figure 4 Responsivity (left) and offset (right) maps for MW2 (longer) band

Measured for the shorter and longer band respectively. Combined with noise levels of 1.4 and 1.7 counts for the two bands, NEDT's of 33 and 24 mK were calculated for the respective bands. Responsivity uniformity was found to be 5.5% and 3.5% (sigma/mean) for the two bands. These results are in good agreement with earlier characterization of similar arrays.

Because post correction uniformity plays an important role in determining the quality of color fused imagery, extensive characterization of FPA performance was carried out in this area. FPA output was offset and gain corrected using two point blackbody calibration at 25 and 35 C. Maps of the gain and offset coefficients are shown in **Figures 3** and **4**. Responsivity coefficients show a near random distribution, with a few extended features. The two dark extended features evident in both bands correspond to faintly visible

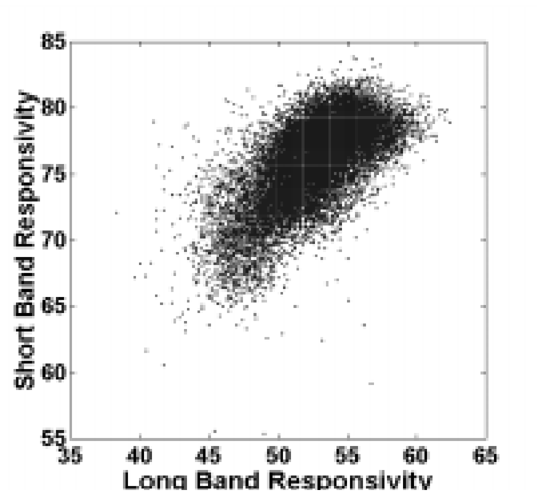

Figure 5 Responsivity scatter plot

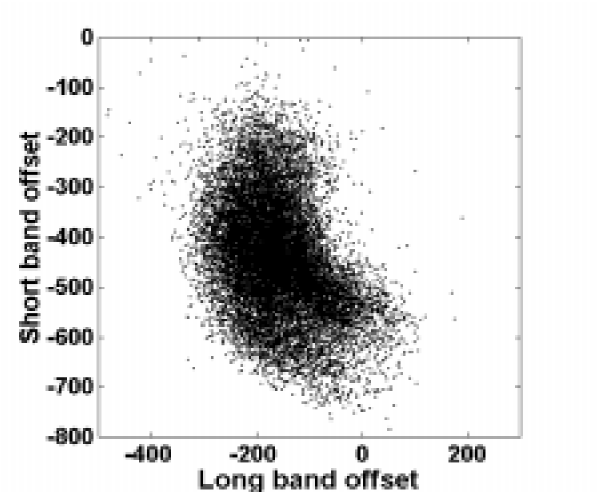

Figure 6 Offset scatter plot

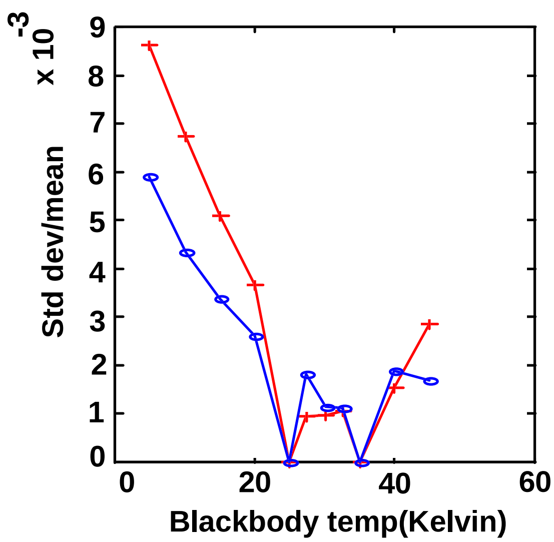

Figure 7 Post correction spatial noise as a function of background temperature

defects on the CdTe side of the FPA. The offset coefficients show a cross hatched pattern aligned with the FPA rows and columns, with superimposed randomly distributed bright individual pixels. In the longer band, these occasionally correspond to pixels with large low frequency noise, or blinkers. No evidence for such behavior is observed for the shorter band. Scatter plots of the responsivity and offsets for each band are shown in **Figures 5** and **6**. Some degree of correlation between the bands for both coefficients is clearly evident, suggesting a common origin. The alignment and symmetry of the cross hatch pattern suggests that it is dominated by some readout related issue. Post correction spatial uniformity as a function of background temperature for calibration points of 25 and 35 C is shown in **Figure 7**. For scene temperatures from 20 to 40 C, the sigma./mean is < .002, or approximately twice the temporal noise.

3.0 COLOR PROCESSING - HARDWARE IMPLEMENTATION

The color display algorithms to be described below have been implemented on a Matrox Genesis PCI bus frame grabber card in a 200 MHz Pentium Pro based PC. This frame grabber captures the nonstandard format 12 bit digital output from the camera head over a 16 bit parallel RS422 bus. Because all image processing, as well as image display functions, are performed on the frame grabber card, neither processing power or bus speed of the host machine are critical in reaching the achieved performance. Image display is via a 24 bit RGB look up table to a dedicated VGA display. This signal has also been converted to RS170 video format for recording on standard VHS video tape. 16 bit integer arithmetic calculations are performed using the TI C80 digital signal processing chip (single processing node configuration) on the card. The processor is capable of up to 2 billion RISC like operations per second. The processor also includes a 100 MFLOP floating point unit. 16 bit integer arithmetic is maintained until the last step in the display process to maintain the full dynamic range of the data, without clipping or digital wrap around effects. Basic arithmetic array functions are accessed using C language library routines that are supplied with the card. Array sums, differences, products, and logical operations are performed real time, at a rate consistent with 60 Hz frame rates and a 128x128 array. The frame grabber architecture is such that additional processing nodes could be added to

Table 1 Processing times for a variety of functions	Time
16 bit integer addition of scalar to 128x128 array	<1.2 msec
16 bit integer scalar multiplication of 128x128 array	<1.2 msec
16 bit integer scalar division for 128x128 array	<2.7 msec
16 bit integer subtraction two 128x128 arrays	<1.2msec
16 bit integer multiply(2 factors) and add with integer arrays	<1.2 msec
16 bit integer look up table mapping 128x128 array	<1.4 msec
3x Zoom of 128x128 array	<2.2 msec

work in parallel, to supply the throughput required for larger format arrays. No low level programming of the C80 is required to implement the desired algorithms. Processing speeds achieved for a variety of functions, including overhead time to make the measurement, is shown in Table I.

4.0 INFRARED COLOR MECHANISMS

Infrared photon flux emitted by a surface at some wavelength is a function of its temperature (as defined by the Planck distribution law) and its surface emissivity. Natural variations in surface temperature and emissivity both contribute to variations in the overall photon flux emitted from any surface. Even for closely spaced bands, these variations can provide the basis for color imagery. During daytime imaging in the midwave bands, there is also a significant contribution to the scene from reflected solar radiation. This becomes an additional source of color as a result of reflectivity differences, and the very different spectral distribution of the 6000K illumination, from the near 300K self emitted radiation. When imaging a target at ambient temperature in background clutter with a single band infrared sensor, the target can appear to have either a positive or negative contrast. Furthermore, using a monochrome display, there is the additional limitation that a human viewer has an instantaneous dynamic range equivalent to only 100 shades-of-gray (a one percent contrast difference). Therefore, for scenes with high background clutter, targets can be hard to discriminate because of confusing contrast inversion possibilities, or the probability that the target and the local background could have zero contrast.

The goal of two band IR color fusion is to overcome the contrast limitations that exist with single band imagery.[3] By using two infrared bands to create a color space, an associated composite color image can be created for display to human viewers. In so doing, the likelihood of detection is increased because *either* the target's brightness *or* color can be different from the background. In this regard, discriminating targets from backgrounds using *IR color fusion* is very similar to color-and-shape discrimination in human color vision. The power of this approach is that it leverages the known human ability to discriminate millions of colors defined by varying hue, saturation, and brightness.

5.0 COLOR DISPLAY ALGORITHMS

.Because the human color vision system has three types of photoreceptors (namely red, green and blue cones), viewing two band imagery is a not a perfect fit. The human color processing system works with color opponents (namely red-green and yellow-blue color opponency). With this understanding, it is possible to use a variant of this to display a two band infrared image. In the work done at NRL, a red-green color opponency was chosen. In practice, the longer spectral wavelength infrared band was input to a red display channel and shorter wavelength band was input to *both* the green and the blue display channels. The combination of equal amounts of green and blue creates cyan. In essence this is the same as what is known as human red-green color opponency. Red and cyan are true color opponents because when they are combined in equal quantities, they create the perception of white, black, or some shade of gray. In this manner the relative intensities between the two bands at each pixel can be represented as a chromatic continuum starting as red, going through gray, and ending as cyan. At the same time a brightness value can be assigned in an orthogonal direction (**Figure 8**). Therefore, each pixel has a chrominant value (red-cyan) and a brightness value (black-white). It is interesting to note that if the data has a large dynamic range in either the brightness or chrominant directions, then a nonlinear compression technique (such as histogram equalization) can be employed in that coordinate system without a major distortion of color values as might occur when performing compression in the original coordinate system.

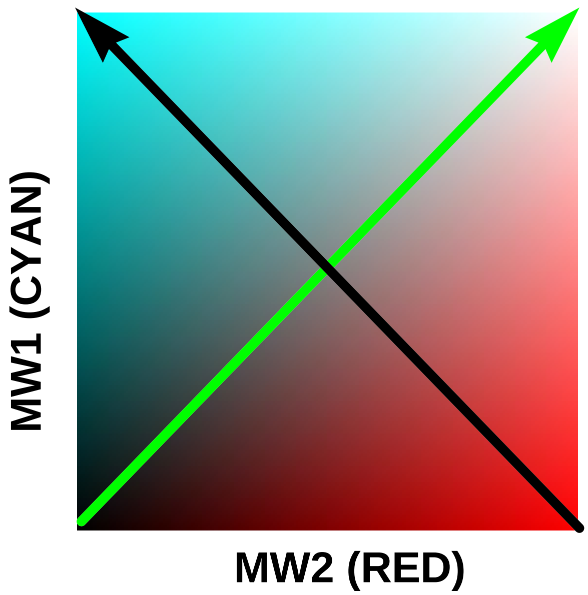

Figure 8 Red-cyan color space. Brightness direction shown green arrow, chromaticity by black arrow.

Two important issues arise when processing two band infrared imagery to create good composite color imagery. The first is that of obtaining good color contrast between objects and backgrounds. The second is obtaining good color constancy regardless of illumination and temperature – that is, target and background colors should be the same at night as during the day, or the same regardless of whether the object is hot or cold. The brightness or the darkness of the object may vary, but the color (hue and saturation) should remain the same. In this paper only color contrast enhancement will be discussed. The issue of color constancy is more complex and will be the focus of future real time imaging demonstrations.[4]

In summary, the approach to color fusion is to map the raw image data into an appropriate color space, and then processing it to achieve an intuitively meaningful color display for a human viewer. The resulting imagery should provide good color contrast between objects and backgrounds and consistent colors regardless of environmental conditions such as solar illumination and variations in surface temperature. The algorithm effort at NRL has focused on attempting to first understand the underlying infrared phenomenology and then apply traditional, linear color processing techniques as appropriate. After this approach is fully explored it may be useful to expand into the area of nonlinear processing. But for the present there remains a great deal to understand.

The fundamental color mechanisms are exhibited in the following laboratory data, where straightforward assignments of the longer wavelength and shorter wavelength data to the red and cyan color planes are made. In this process, linear scaling, based on the statistical properties of the data for each band, is applied to each band to normalize the data to have common means, and maxima. The transmission spectra for a sheet of polystyrene, (round object in the image) and teflon ,(square object in the image) each approximately 1 mm thick are shown in **Figure 9** The teflon can be seen to be more transparent in the shorter wave band, and less transparent in the long wavelength band, with the polystyrene behaving just the opposite. **Figure 10** shows fused color imagery including the two objects. When backlight with a blackbody source, the teflon appears as cyan, while the polystyrene appears as red. When the objects are heated slightly above ambient and held in front of a dark background, then the signature is dominated by emission, and the teflon appears red and the polystyrene appears cyan. A signature which is a combination of transmission and emission characteristic can be observed where the warm objects are backlight with a warm blackbody source (finger) as well.

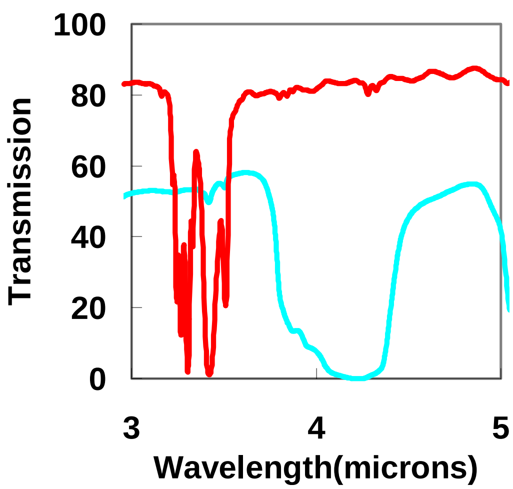

Figure 9 Transmission of polystyrene (red) and teflon (cyan)

Figure 10 Polystyrene (round) and teflon (square) sheets in transmission and emission

.One problem that typically arises when mapping infrared data into a color space is that the corresponding pixel values between two bands are often highly correlated for those infrared wavelengths that are predominantly self-emitting. This is particularly true of any sub-bands in the MWIR and LWIR spectral bands at nighttime. Note that other infrared regions such as the SWIR and NIR spectral bands are predominately used in daytime imaging systems that view solar-reflected photons. The correlation between two MWIR bands for a night scene is shown in **Figure 11**. The distribution of pixel values tends to be a locus of points that runs diagonally through the scatter plot of the original color space. Simple scaling or normalizing of each band individually results in the image in **Figure 12,** which displays relatively little color content other than the CO2 emission related signatures from the smokestacks from the power generating plant.

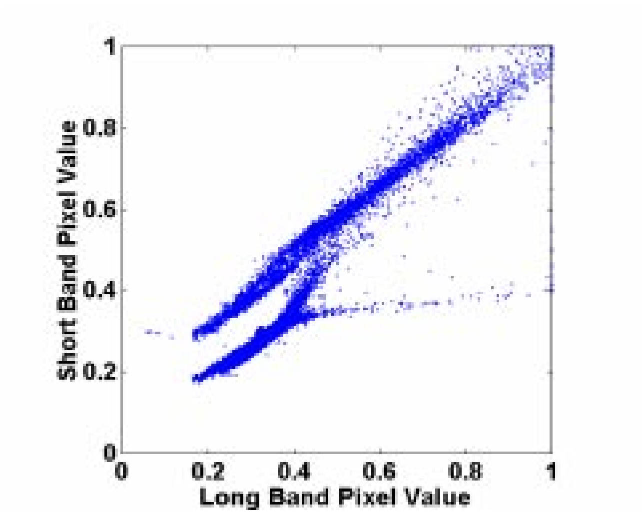

Figure 11 Scatter plot for correlated scene shown below

.Color contrast enhancement can be achieved using a two-step process. First, a new coordinate system is established where the primary axis is in the brightness direction and a secondary, orthogonal axis in the chrominant direction. The primary axis (or *principal component direction*) is based on the pixel statistics. In the most general formulation, this is computed by finding the covariance matrix of all the pixel values and then finding the eigenvectors of the covariance matrix. Using the eigenvectors of the largest eigenvalue (which relate to the principal component direction for correlated data) a rotation matrix can be found that translates the values from the original coordinates into the new coordinate system. The principal component direction is taken to be the brightness direction, and the chromaticity direction is orthogonal to it. The new coordinate system (with one axis being a principle component direction) is very useful because it allows certain types of color processing to be performed in a separable manner. For example, because the two bands are highly correlated, the pixel values tend to lie near the principal coordinate axis, whereas if the data is uncorrelated it will tend to have a circular distribution. Correlated data can be de-correlated in the transform space to achieve color contrast enhancement. That is, the luminance and chromimance values data can be re-scaled separately in the new coordinate system, then rotated back into the original coordinate system, resulting in decorrelation of the

Figure 12 Fused color image formed by linear scaling of each band

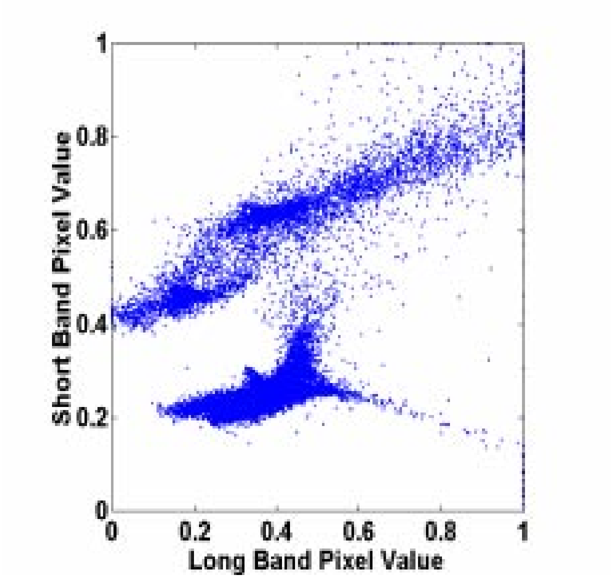

Figure 13 Scatter plot after decorrelation for image shown adjacent.

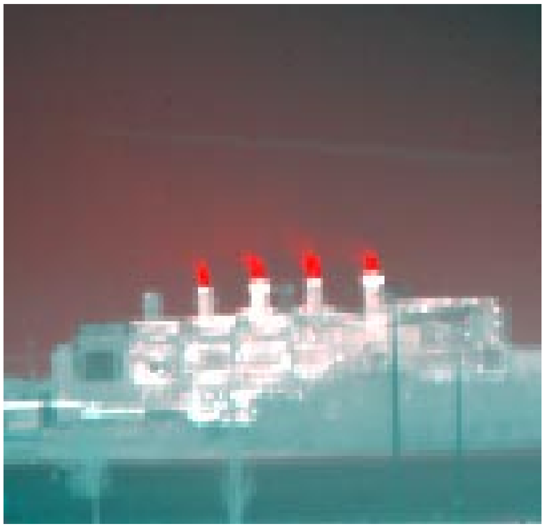

Figure 14 fused color image after decorrelation

original data. In practice, the principal component direction has been assumed to be at 45 degrees to the red and cyan axes. In simplified approximation, the brightness is then the sum of the short and long band pixel values, and the chrominance is the difference of the short and long band values. Color enhancement is achieved by multiplicative scaling of the chrominance data, followed by transformation back to the red-cyan color space. In the inverse transformation, red is the difference of the brightness and color, and cyan is the sum of the brightness and color. An example of decorrelated image data is shown in **Figure 13 and 14**.

Under solar illumination, the principal component axis no longer lies equidistant between the red and cyan axes because of the lack of correlation between the two bands. The algorithm

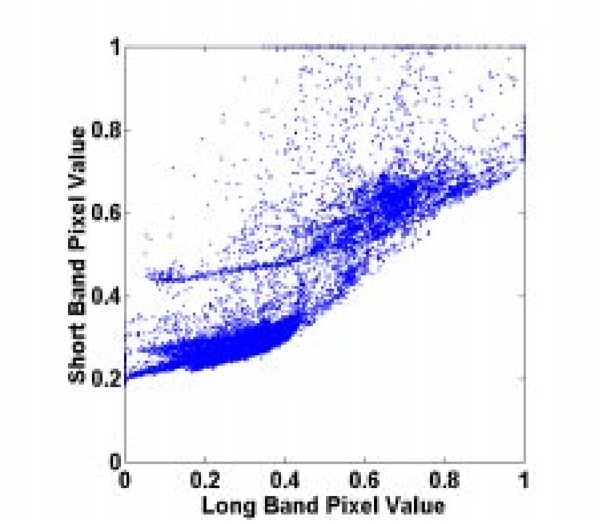

Figure 15 Scatter plot for strongly uncorrelated image dominated by solar reflections

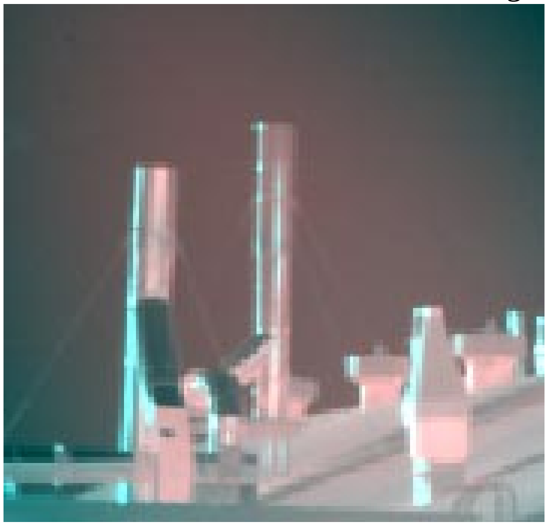

Figure 16 Fused color image with strong solar reflection component

described above produces unpredictable color balance under those conditions. Because the correlation between the bands is weak however, significant color contrast can be achieved using simple scaling of the information from the two bands. Such an image is shown along with its scatter plot in **Figures 15** and **16**. Solar reflections are clearly indicated by the strong cyan components visible in the image.

.In a heavily correlated scene, where some pixels which lie just beyond the edge of the distribution for the rest of the scene, it is possible to identify those pixels by applying a thresholding function to a difference of the two bands. This identification can then be used to key these pixels to a unique color with large contrast to the rest of the scene. This can occur when a relatively dim long band source, e.g. low level CO2 emission from a butane lighter is back-light with a hot blackbody source (**Figure 17a**). Strong color contrast may be regained by using the difference information as a key to turn off the green and blue components of a pixel which exceeds the threshold **(Figure 17b**). Although this approach does not result in a 'realistic' color image, it provides a clear visual cue to a signature of interest.

Figure 17a & b Highly correlated image with weak MW2 signal before and after difference/threshold process

Figure 18 shows an image obtained by a uniform histogram equalization of each band independently prior to assignment of colors. The image has the advantage of displaying the full dynamic range of the scene with strong color contrast. However, it has the disadvantage discussed earlier of resulting in wide variations in color from scene to scene, depending on what reference is used for the equalization. Future plans include using this approach in the chrominance-brightness space to achieve improved color contrast, with good constancy.

Figure 18 Histogram equalization per band image.

Because the de-correlation routine involves the sums and differences of the two bands, both temporal and fixed pattern noise is magnified. This problem is magnified by the fact that the spatial noise for the two bands is correlated to some degree. Fixed pattern noise typically limits the extent to which the color can be enhanced without degrading the quality of the image. An example of very high brightness and high color gain image is shown in **Figure 19.** The observed noise is nearly all the result of fixed pattern effects rather than temporal noise.

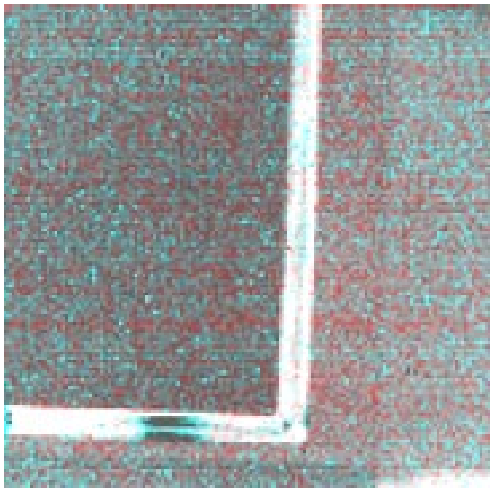

Figure 19 Fixed pattern noise under high contrast and color gain conditions.

6.0 SUMMARY

Real time implementation of a variety of color fusion algorithms has been demonstrated with a simultaneously integrating co-located two color midwave IRFPA. Along with providing visual cues for spectral sharp signatures associated with CO2 emission, good color contrast has been achieved for both night and daytime imagery. While sensor NET is degraded over either single band NET, by amplification of both temporal and fixed pattern noise in the color generation process, the additional information provided by color compensates in part for this in target identification.

7.0 ACKNOWLEDGEMENTS

The authors thank Jerry Wilson and associated staff at SBRC for helpful discussions on FPA related issues, and Mark Stegall of SEIR for camera related discussions. This work was supported by ONR under the NRL 6.2 base program work unit 68-6383.

---

[1] K. Sarkady, et.al., "Performance Evaluation of a Staring Two Color Missile Approach Warning System," IRIS Meeting on Infrared Countermeasures, Laurel, MD (April 95) and publication in Proceedings Vol III, p 243, March 96.

[2] J. Caulfield, J. Johnson, E. Patten, P. Goetz, A. Estrada, S. Solomon, J. Wilson, S. Johnson, R. Wyles, R. Rajavel, J. Jensen, D.Jambam "Simultaneous Integrating Staring Two Color IRFPAs," "Proc. 1997 IRIS Detector Specialty Group Mtg., p.351 (Feb. 1998).

[3] D. A. Scribner, J. Schuler, M. P. Satyshur, S. P. Michaels, and M. R. Kruer, "IRFPA Requirements for Dualband Imaging Sensors," Proc. 1996 Meeting of the IRIS Specialty Group on Infrared Detectors, p. 383, 31 July 1996 (pub. May 1997).

[4] D. Scribner, J. Schuler, P. Warren, M. Satyshur, M. Kruer, "Infrared color vision: separating objects from backgrounds", Proceedings of the SPIE – Infrared Detectors and Focal Plane Arrays V, Conf. No. 3379, April 1998.